Supramolecular Chemistry
Vol. 24, No. 5, May 2012, 333–343

Synthesis, characterisation and photoswitchability of a new [2]rotaxane of α-cyclodextrin with a diazobenzene containing π-conjugated molecular dumbbell

Ioanna Deligkiozi[a], Raffaello Papadakis[a,b] and Athanase Tsolomitis[a]*

[a]*Laboratory of Organic Chemistry, School of Chemical Engineering, National Technical University of Athens (NTUA), 15780 Athens, Greece;* [b]*CNRS, Université Paul Cézanne, UMR6263, ISM2/BiosCiences, Marseille 13397, France*

(*Received 4 November 2011; final version received 19 January 2012*)

In this work, a new [2]rotaxane consisted of a diazobenzene containing π-conjugated linear compartment, including the 4,4′-bipyridyl moiety and α-cyclodextrin (α-CD) as the macrocyclic compartment, was synthesised with yields of nearly 57% and fully characterised. α-CD easily assembled with the linear compartment and suitable bulky ends (stoppers) in water to give a new [2]rotaxane. The characterisation of this supramolecular compound was accomplished using several spectroscopic techniques such as ^{1}H NMR, ^{13}C NMR and 2D NMR spectroscopy, powder X-ray diffraction, fourier transform infrared spectroscopy, induced circular dichroism and UV–vis spectrophotometry, as well as scanning electron microscopy and Energy Dispersive X-ray. Furthermore, the reversible E–Z photoisomerisation of both [2]rotaxane and its molecular dumbbell was investigated by irradiation with UV light.

Keywords: α-cyclodextrin; molecular switches; [2]rotaxane; diazobenzene; viologens

Introduction

Rotaxanes are a relatively new class of nanomaterials (*1–3*), which have been intensively investigated in the last two decades because of their ability to act as molecular switches by giving controllable, reversible transformations (*4*, *5*). These are materials consisting of one or more linear molecular fragments, and one or more macrocyclic molecules threaded through the first ones, and stoppered with suitable side bulky moieties (the so-called stoppers) (*6–8*). Many attempts have been made in the past and have yielded in challenging rotaxanes and pseudorotaxanes, with potential applications in nanotechnology and molecular electronics (*9*, *10*), serving as molecular switches (*11–14*), molecular wires (*15–17*) and molecular memory devices (*18*). [2]Rotaxanes, the structurally simplest rotaxanes, consist of one linear and one macrocyclic compartment as well as two bulky moieties at both sides of the linear part, preventing the macrocyclic molecule from slipping away, hence stabilising the inclusion complex. A very interesting class of rotaxanes includes the inclusion complexes of suitable linear molecules with cyclodextrins (CDs). CDs are structurally 1 → 4-α-linked anhydroglucopyranose cyclic oligomers and have the geometry of truncated cones, the cavities of which are hydrophobic and they can easily create inclusion complexes by self-assembling with a wide class of organic molecules, including many aromatic and other compounds (*19*, *20*).

In this work, α-cyclodextrin (α-CD) has been used for the preparation of a new [2]rotaxane, interacting by self-assembling, with a new synthesised linear molecule. What is interesting with this [2]rotaxane is that its linear molecular part presents high π-conjugation. Several works have been published in the past concerning the use of conjugated (either polymeric or oligomeric) compounds for the preparation of molecular wires due to their electrical conductivity attributed to their conjugation (*15–17*). Herein, we report the synthesis of a new [2]rotaxane with such a linear compartment.

Additionally, it is known that diazobenzene-based compounds can easily undergo a reversible E–Z isomerisation of the type shown in Scheme 1. Since, the Z diastereomer is more unstable than the E one, the energy needed for E → Z isomerisation is higher than that needed for the Z → E isomerisation. Consequently, the first one occurs photochemically whereas the second one thermally.

This is the reason why diazobenzene-based ‘linear’ molecules have been used in the past for the preparation of switchable rotaxanes (*11*). This controllable isomerisation can lead to the movement of the threaded macrocycle (in our case α-CD) to another position due to stereochemical reasons, in other words the CD moiety can shuttle between the azo group in response to an external stimulation, e.g. UV light. Thus, a diazobenzene [2]rotaxane can act as a molecular shuttle. In this work, they are used for the same reason, and shuttling of α-CD in the case of the synthesised rotaxane is investigated.

---

*Corresponding author. Email: tsolom@chemeng.ntua.gr

ISSN 1061-0278 print/ISSN 1029-0478 online

http://dx.doi.org/10.1080/10610278.2012.660529
http://www.tandfonline.com

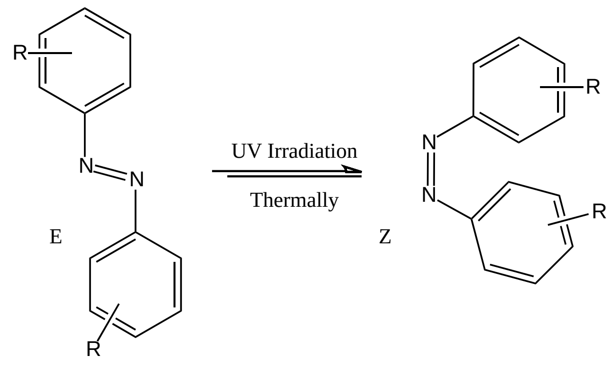

Scheme 1. Switchability of a diazobenzene derivative.

Results and discussion

Synthesis

In this work, we report the synthesis of a new [2]rotaxane with a π-extended conjugated linear compartment. Several works have been published in the past concerning [2]rotaxanes without conjugation in their linear compartments. Although the high conjugation induces several interesting properties such as conductivity or semiconductivity to the final material, little has been done in the field of rotaxanes which contain highly conjugated compartments, due to possible difficulties in their synthetic procedures.

For the preparation of the title [2]rotaxane, first of all the 'linear' compound **2** (Scheme 2) had to be synthesised. For that purpose 4-(2,4-dinitrophenyl)-4′-bipyridinium chloride **1** (a Zincke salt) was used as the starting material synthesised according to procedures published in the past (*22*, *23*) to give after a Zincke reaction with 4,4′-azodianiline (ADA), in the solid phase the precursor (new product) linear compound **2** as shown in Scheme 2. This is a reaction which in our hands did not yield compound **2** in solution. However, it is remarkable that in the solid phase this reaction is more favourable probably because of the removal of the 2,4-dinitroaniline (leaving group) through sublimation.

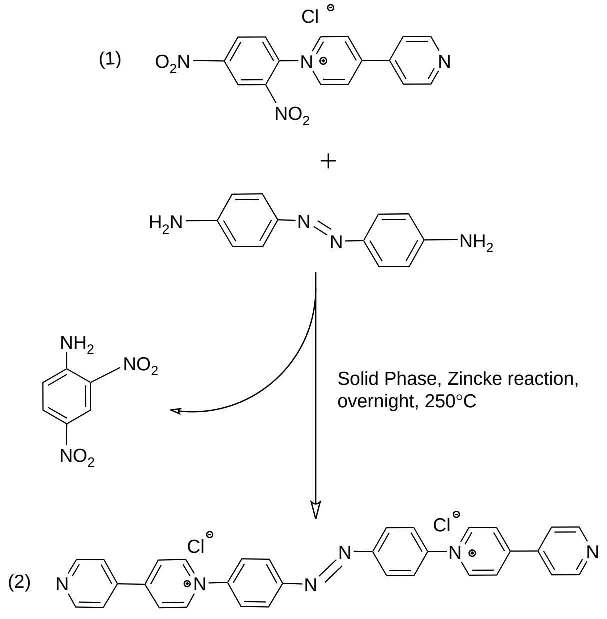

Scheme 2. Synthesis of linear compound **2**.

Compound **2** was then reacted with an excess of fluoro-2,4-dinitrobenzene and α-CD in water to yield through a self-assembling 'threading' reaction of the desired [2]rotaxane.

The threading technique is a widely used synthetic strategy for rotaxane synthesis (*24*) during which a pseudorotaxane is initially formed. The pseudorotaxane corresponds to the inclusion complex of α-CD with the linear compound **2**.

This complex is not stabilised with any side bulky substituent; that is why it is relatively unstable. In the presence of an excess of fluoro-2,4-dinitrobenzene, the as-formed pseudorotaxane is transformed to the desired [2]rotaxane. The 2,4-dinitrophenyl moieties are bulky enough concerning the dimensions of α-CD, which is the smallest CD (*19*), to prevent decomposition of the rotaxane.

As depicted in both Schemes 3 and 4, the compounds **3a** and **4a** (salts with counter anions Cl^- and F^-) were transformed to the corresponding hexafluorophosphates **3b** and **4b** (salts with counter anions PF_6^-) via an ion exchange reaction of **3a** and **4a** with the salt NH_4PF_6.

The reason why this ion exchange reaction was chosen is that as reported in the past (*25*), the hexafluorophosphate salts of viologens (substituted 4,4′-bipyridines) are soluble in various polar organic solvents (Acetonitrile, Dimethyl sulfoxide (DMSO), Dimethylformamide, acetone, etc.) whereas the halogen (F^-, Cl^-, Br^-) salts of viologens are soluble in water but insoluble or slightly soluble in organic solvents. Consequently, this helped to easily dissolve the compounds **3b** and **4b** to suitable solvents for the needs of characterisation.

The dumbbell compounds **4a,b** (Scheme 4) were also synthesised to help the interpretation of the structure of the [2]rotaxanes **3a**,**b**, by comparing their spectral features. For the synthesis of the compounds **4a**,**b**, the same conditions as those used for the synthesis of the [2]rotaxanes were chosen.

Characterisation

For the characterisation of the synthesised compounds, several spectroscopic techniques were employed. As mentioned before, the comparison of the spectroscopic data of the dumbbell-like compound **4b** with those of the final [2]rotaxane **3b** made the characterisation feasible. In this work, compound **4b** (the hexafluorophosphate [2]rotaxane salt) has been fully characterised through various spectroscopic techniques, as it will be analysed.

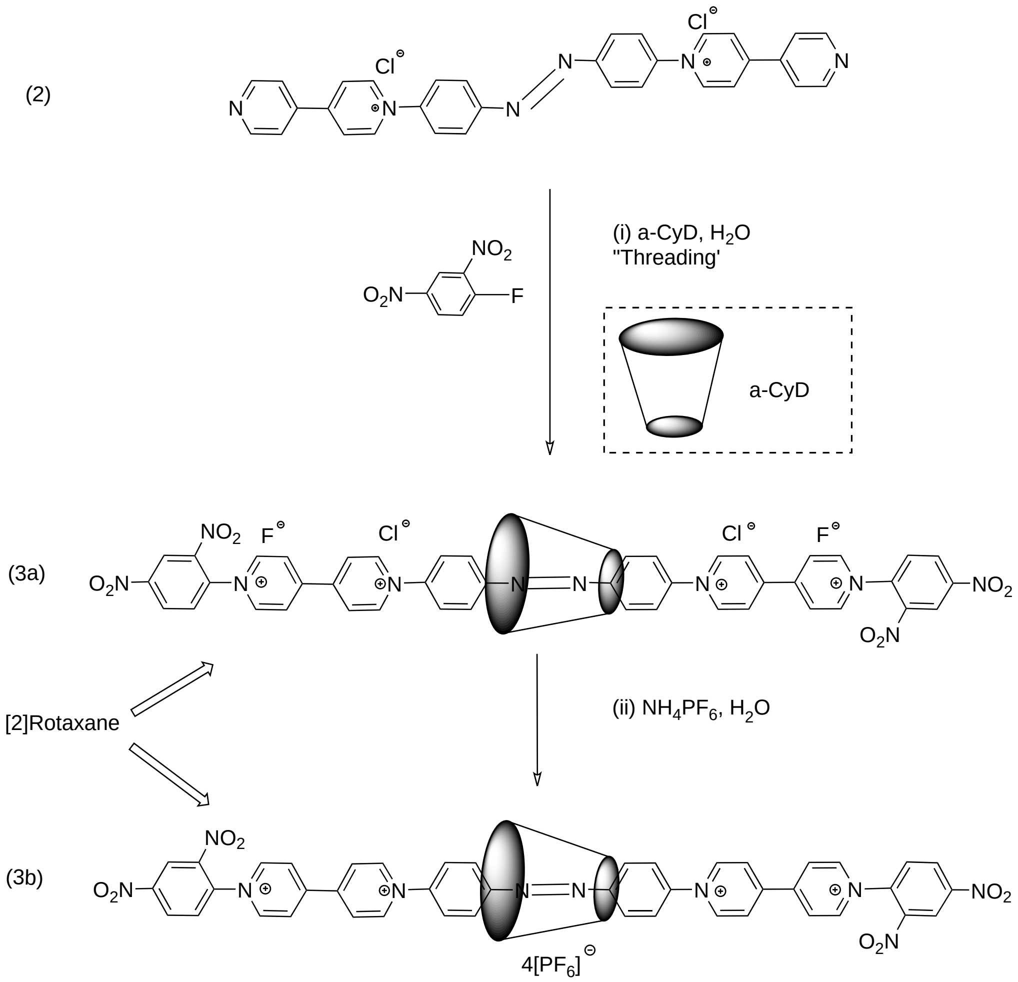

Scheme 3. Synthetic route for the preparation of the [2]rotaxane **3a**,**b**.

^{1}H NMR, ^{13}C NMR and rotating frame Overhauser effect spectroscopy

The formation of the inclusion complex between the dumbbell-like molecule and α-CD is clearly confirmed by ^{1}H NMR, ^{13}C NMR and 2D NMR spectroscopy experiments in D_6DMSO. The NMR study gave clearly strong indications that an interaction between the dumbbell compound and α-CD takes place (Figure 1; Figures S1 and S2 of Supplementary Information, available online).

This result supports the formation of the [2]rotaxane structure. It is also observed that the interior H^3 and H^5 protons located in the internal α-CD cavity, shifted upfield as expected (Figure S1 of Supplementary Information, available online) which indicates that these signals are strongly sensitive to the electronic environment inside the cavity with the aromatic phenyl protons b and a of the dumbbell molecule (Scheme 5) (*26*).

Taking into account the proportion of the protons of α-CD and of the protons of the dumbbell molecule, obtained from the relative integrals of the NMR spectra of **3b**, it is easily deduced that both these two components are assembled in equimolar proportion in the [2]rotaxane molecule **3b**. Additionally, the corresponding neighbourly protons of the quaternary nitrogen atoms lose their symmetry due to the presence of α-CD. This is a strong evidence of the formation of an inclusion complex (*27–30*) (Figure S2 of Supplementary Information, available online).

Furthermore, a broadening of almost all aromatic and α-CD peaks was observed which is probably attributed to the interaction of the two compartments of the inclusion complex **3b**. Concerning the ^{13}C NMR spectra, it has been observed that for the case of **3b** both the carbon atoms of α-CD and of the dumbbell compound are present (see ‘Experimental’ section).

To obtain more detailed information, the stable conformation of the [2]rotaxane was additionally fully characterised by 2D ^{1}H rotating frame Overhauser effect spectroscopy (ROESY), which is depicted in Figure 1. 2D NMR spectroscopy has recently become an important method for studying the structures of CD-containing rotaxanes, since one can conclude that two protons are

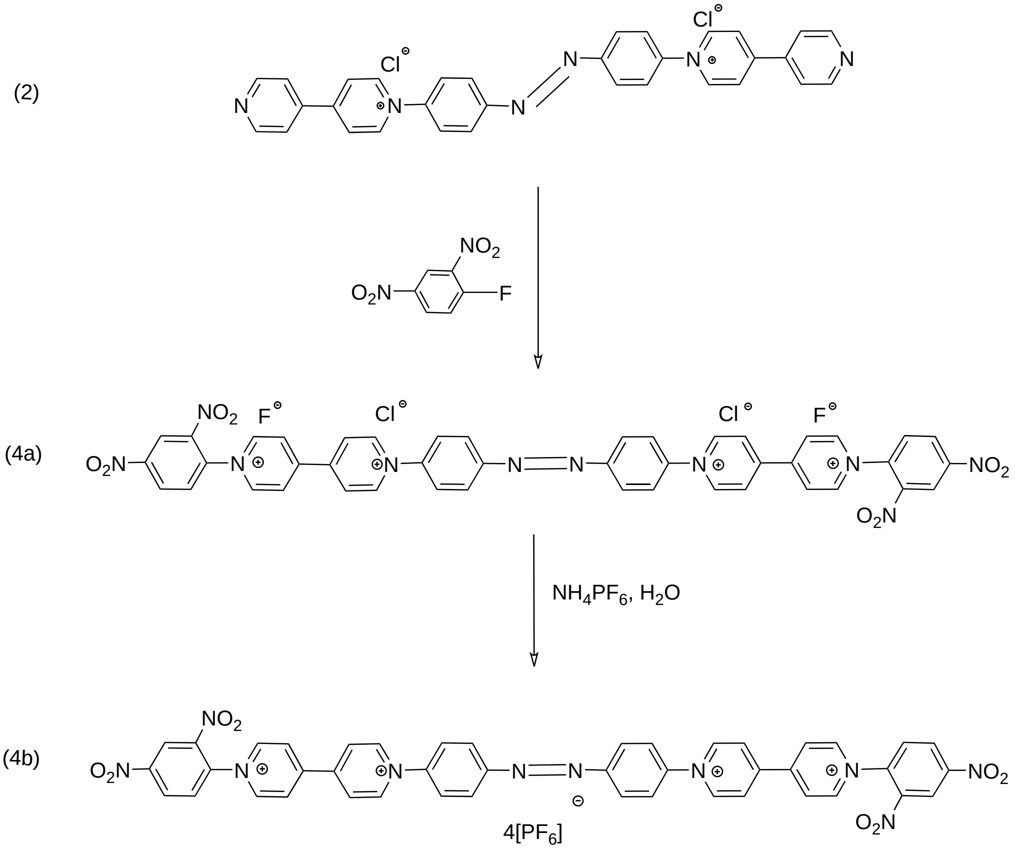

Scheme 4. Synthesis of the dumbbell-like molecules **4a**,**b**.

closely enough located in space if a cross-peak is detected between the relevant proton signals in the rotating frame Overhauser effect (ROE) spectrum.

In the ROE spectrum of Figure 1, the cross-peaks of α-CD and the aromatic phenyl protons a and b (Scheme 5) are clearly shown, and that corresponds to the fact that the α-CD ring is located around the azobenzene unit, an additional evidence that the aromatic guest is included in the CD cavity between the interior H^3 and H^5 protons.

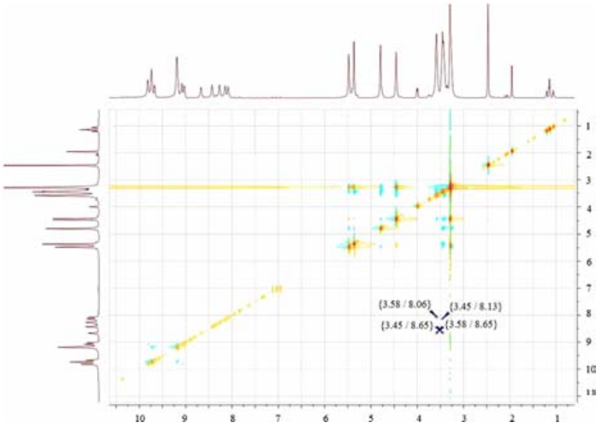

Figure 1. The 2D ^{1}H ROE NMR spectrum of **3b** ([2]rotaxane), 600 MHz in D_6DMSO at 298 K; mixing time 300 ms.

Determination of the structure in solution

2D ROESY experiments provided us with the information on the averaged relative inter- and intramolecular proton distances, for the closeness between the dumbbell compound and α-CD. In the 2D spectrum of Figure 2, intense cross-peaks are observed between the aromatic protons of the dumbbell compound and those of the inert protons of the CD cavity (H^3, H^5) as it was noted previously. The relative volumes of the most important cross-peaks have been summarised in Table S1 (Supplementary Information, available online). No correlation is detected between the dinitrophenyl group and any of the α-CD protons and this fact indicates that the stoppers of the molecule are placed outside the cavity.

X-ray diffraction

The powder X-ray diffraction (XRD) is a method generally used to characterise CD-based complexes, because the patterns of these compounds are different from those of the native CDs. The XRD pattern of the dumbbell compound differs from that of the [2]rotaxane. Additionally, they both

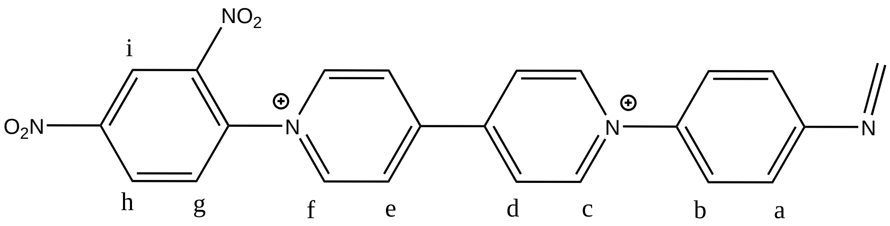

Scheme 5. Designation of hydrogen atoms for compounds **3** and **4**.

differ from the diffraction pattern of the free α-CD. The diffractogram of α-CD has shown intense and sharp peaks, indicating its crystalline nature. The α-CD shows characteristic reflections at $2\theta = 12.2, 14.3, 21.7, 13.5, 5.3$ and 9.7°. In contrast, the dumbbell compound shows a few sharp peaks with characteristic reflections at about $2\theta = 21.5, 20.1, 26.9, 23.5, 39.6$ and 10.8° having less intensities (Table S2 Supplementary Information, available online). This fact indicates the semi-crystalline nature of the dumbbell compound. However, these characteristic reflections disappeared in the case of the [2]rotaxane (**3b**), indicating that the arrangement of α-CD in the complex ([2]rotaxane) is modified after the rotaxanation. Additionally, the inclusion complexes of α-CD with the dumbbell compound showed undefined, broad, diffused peaks with low intensities. The diffraction pattern of the [2]rotaxane (**3b**), exhibits a wide-spreading peak from $2\theta = 10$–30°. All the samples were analysed in the 2θ angle range of 5–60° (Figure 3).

Scanning electron microscopy (SEM) observations, depicted in Figure 4, gave some insights concerning the different morphology of the synthesised compounds. SEM experiments were carried out on all compounds, as shown in Figure 4(a)–(c). When the magnification of SEM was × 400, the morphologies of α-CD and the compounds **3b** and **4b** were different (for better resolution, see also Figure S6 of Supplementary Information, available online).

As shown in Figure 4(a), the morphology of α-CD corresponds to aggregates of crystalline grains of irregular form with the size varying from 20 to 100 μm. On the other hand, the dumbbell compound is a semi-crystalline material and finally the [2]rotaxane (Figure 4(b),(c)) is amorphous. Additional evidence of the successful rotaxanation has been obtained through the Energy Dispersive X-ray (EDX) measurement (elemental analysis) of the compounds **3b** and **4b** (Figure S6 of Supplementary Information, available online). The elemental analysis is in agreement with the expected one for the rotaxanated dumbbell compound **3b**.

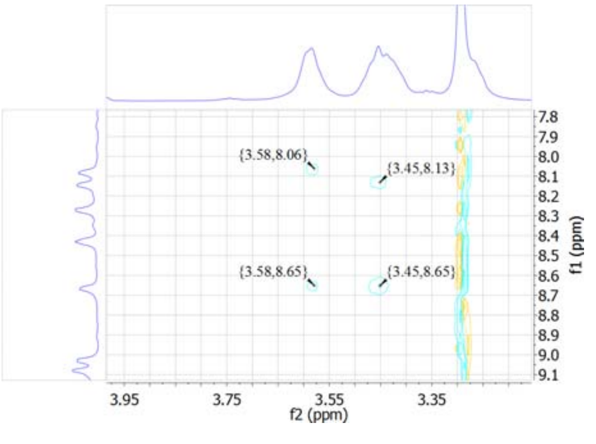

Figure 2. Partial view of ROE corresponding cross-peaks.

Mass spectroscopy

The mass spectra of the [2]rotaxane and the dumbbell compound were also confirmed by their MALDI-TOF-MS and ESI-HR-MS. The structure of the [2]rotaxane under investigation was confirmed additionally by ESI mass spectrometry. In the mass spectrum of the [2]rotaxane salt, the molecular ion corresponds to the tetra-anion formed by the loss of four hexafluorophosphate anions. Figure S3 of Supplementary Information, available online, shows the mass spectrum of the [2]rotaxane, in which the corresponding peaks are listed. The mass spectra showed peaks at *m/z* values for $M{-}4PF_6 + 1H$, corresponding to the loss of four hexafluorophosphate counter ions. In the case of the dumbbell compound, peaks at *m/z* values were observed, corresponding to the loss of four hexafluorophosphate counter ions $M{-}4PF_6 + 1H$. Additionally, in the case of the [2]rotaxane, major fragment ions like the dumbbell compound and the α-CD were observed.

UV–vis spectroscopic and circular dichroism study

In Figure 5, the UV–vis and induced circular dichroism (ICD) spectra of the dumbbell compound and the [2]rotaxane are shown, all recorded in DMSO. In the UV–vis spectra of both compounds, a broad band in the region 300–400 nm, which is attributed to the π–$\pi*$ excitation of the group ($-N=N-$) (*31*) is observed.

A bathochromic shift of this band is observed when rotaxanation takes place. The maximum wavelength for the dumbbell compound is 337 nm whereas the measured one for the case of the compound **3b** ([2]rotaxane) is 351 nm. This has to do with the intercomponent interaction between the α-CD cavity and the ($-N=N-$) group of the dumbbell-like

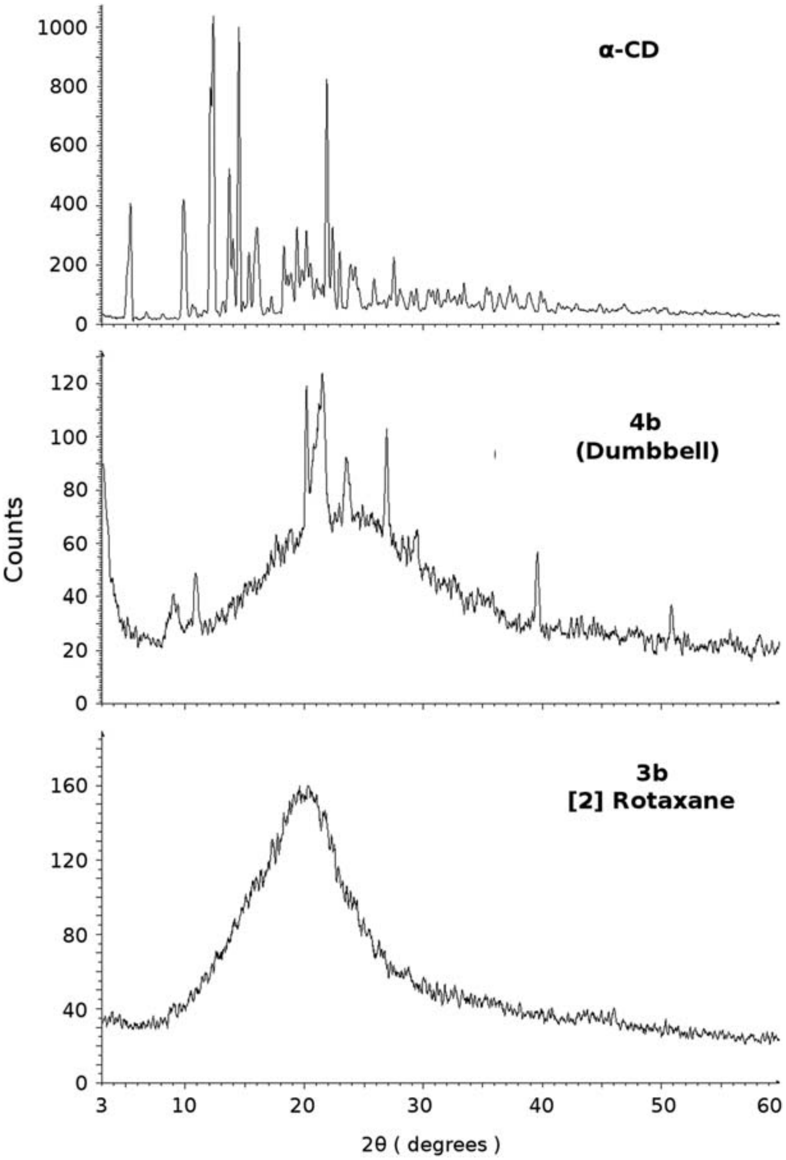

Figure 3. XRD patterns of α-CD and of the compounds **3b** and **4b**. Diffraction intensity in arbitrary units.

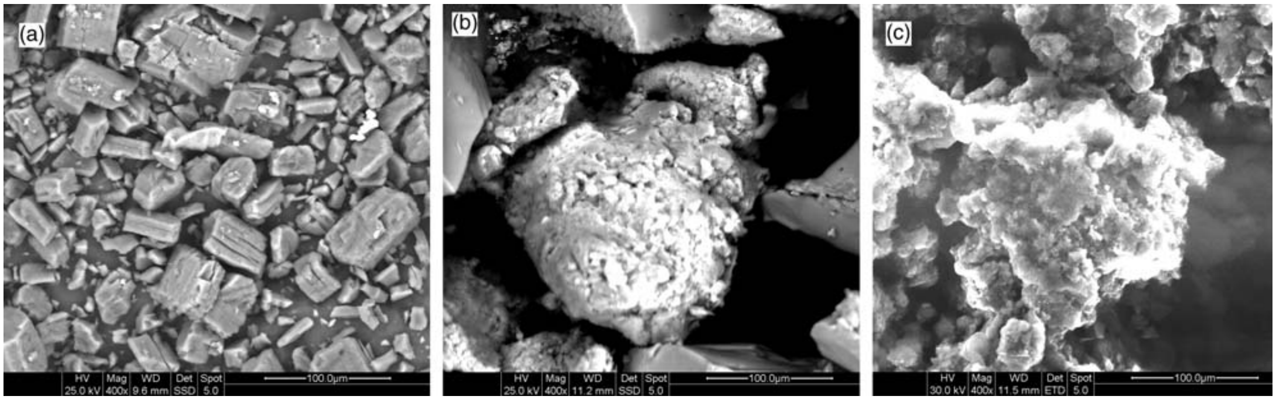

Figure 4. SEM images of α-CD (left), and compounds **3b** (middle) and **4b** (right).

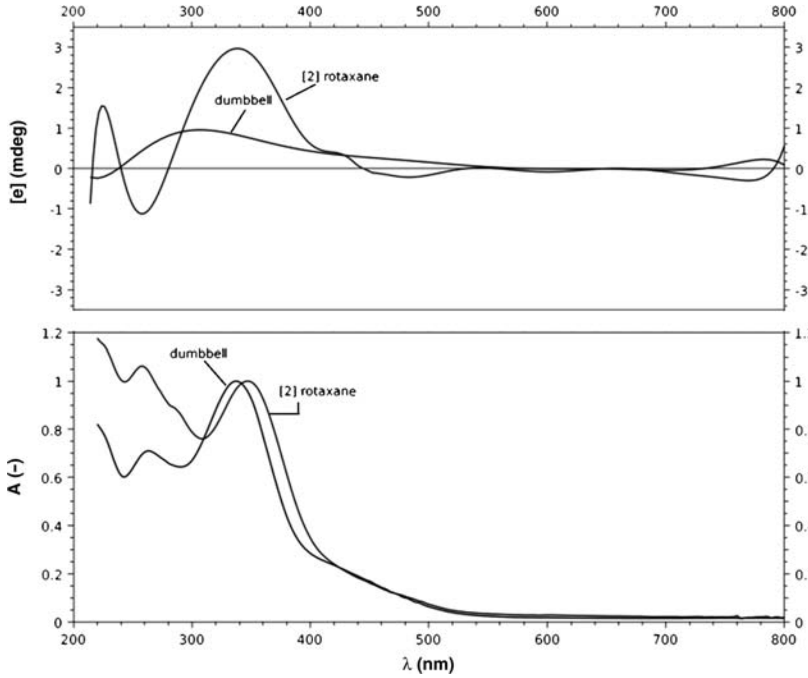

Figure 5. ICD (top) and UV–vis (bottom) spectra of **3b** and **4b**.

compound, which causes a decrease in the energy difference between the ground and excited state of the azo compound. Hence, the energy needed for the $\pi-\pi*$ excitation is lower (bathochromism) (*32*). This 'environment-responsive' character of the $\pi-\pi*$ excitation band of the ($-N=N-$) group has also been observed in solutions of **4b** in different hydroxylic solvents such as ethylene-glycol and methanol (solvatochromic effect).

The ICD spectra of the compounds **3b** and **4b** were different. A characteristic positive band at about 330 nm with molar ellipticity of about 3 mdeg was observed in the case of the [2]rotaxane (**3b**). A shoulder at about 430 nm was also observed as well as a negative band in the region 450–520 nm ($\theta \approx -0.3$ mdeg). These are characteristic features also observed in the case of other relevant [2]rotaxanes with azo-containing viologen-based molecular dumbbells assembled with α-CD (lacking conjugation) (*36*). The situation was much different in the case of compound **4b**. The ICD spectrum of the molecular dumbbell lacks all of the mentioned features and presents a positive peak at about 300 nm with $\theta \approx 1$ mdeg. This is an additional information which reflects the diversity of molecules **3b** and **4b**.

Infrared spectroscopy

Finally, infrared spectroscopy was also employed for the characterisation of the compounds **3b** and **4b**. This spectroscopic technique has been used in the past for the characterisation of [2]rotaxanes since it is a tool to prove the presence of both host and guest components (*33*). In the case of the compounds studied in this work, evidence based on the differences of the fourier transform infrared spectroscopy (FTIR) spectra of the **3b** and **4b** is obtained. As shown in Figure S7 of Supplementary Information, available online, the signals attributed to aromatic absorptions due to the stretching of the ($C=C$) bond and of the azo ($-N=N-$) bond are shifted to higher wave numbers in case of **3b**, due to the interaction of the azo group and the neighbouring aromatic nuclei with α-CD. As observed, the stretching of the ($C=C$) and the ($-N=N-$) bonds become energetically harder, thus the observed increases in the corresponding absorption wave numbers, in case of the compound **3b** are induced. Additionally, a sharp absorption band, noticed at 1484 cm^{-1} due to the pyridine ring stretching vibrations, of the 4,4′-bipyridine moiety of the dumbbell compound, was also reduced about 40 cm^{-1} (1446 cm^{-1}).

Photoswitchability and light-driven molecular shuttle function

Photoswitchable azo-containing molecular shuttles have been studied for several years. Herein, we report the photoswitchability of the [2]rotaxane (**3b**) and the corresponding molecular dumbbell **4b**. As shown in Figure 5, two absorption bands appear in the UV–vis spectra of **3** and **4b**. First of all, a low energy $n-\pi*$ visible band at about 450 nm of low absorbance, which typically appears as a shoulder of a second band of much higher absorbance. The latter corresponds to a $\pi-\pi*$ excitation of the ($-N=N-$)

group, and lies in the ultraviolet region at about 330–350 nm (*34*, *35*). When compounds **3b** and **4b** are irradiated with UV light (as described in the 'Experimental' section), they undergo E–Z isomerisations. In both cases, the E-isomer is more stable than the Z. Thus, visible light or heating of the produced by irradiation Z-isomer, can lead back to the initial more stable E-state (*34*, *36*). In the case of [2]rotaxane **3b**, this photoisomerisation results in the movement of the threaded α-CD molecule to another position ('station') because of hindrance, as also proved by 2D NMR experiments. This E → Z isomerisation which is reversible (*37*, *38*) induces a motion of the described molecular shuttle upon irradiation. A comparison of the E–Z isomerisation, through UV–vis spectrophotometry for the cases of **3b** and **4b**, is shown in Figure 6 and Figures S10 and S11 of Supplementary Information, available online. In both cases a decrease in the $\pi-\pi^*$ band and an increase of the $n-\pi^*$ visible band was observed, indicating the formation of the Z-isomer (*36*, *39*). A slight hypsochromic shift of the $\pi-\pi^*$ band of **3b** upon irradiation and E–Z isomerisation corresponds to the slipping of α-CD away of the (–N = N–) group. (As mentioned, rotaxanation and stoppage of α-CD close to the azo-group cause the bathochromic shift of the $\pi-\pi^*$ band of compound **3b** (Figure S11 Supplementary Information, available online). This was not observed in the same extent for **4b**.

The characteristic $\pi-\pi^*$ and $n-\pi^*$ absorption bands and conversions at the photostationary states of the [2]rotaxane and the dumbbell in DMSO, after 1–6 h of irradiation are summarised in Tables 1 and 2 (plots of E–Z conversion vs. irradiation time, in Figures S8 and S9 of Supplementary Information, available online). E–Z conversions were calculated by the fraction $|A_t - A_p|/A_t$, where $A_t = \pi-\pi^*$ absorbance at trans state and $A_p = \pi-\pi^*$ absorbance at photostationary state (*40*). We have observed that the spectral changes for the dumbbell compound were quite greater (39.33%) than those of the [2]rotaxane (20.54%). This difference in the conversion could be attributed to the fact that it is easier for the dumbbell compound to undergo E/Z photoisomerisation. This is not surprising in contrast with the [2]rotaxane because the isomerisation becomes more difficult in the presence of the α-CD ring (*41*), as described for other similar cases in the past.

Concluding remarks

In summary, in this work, we have described the design, synthesis and characterisation of a new photo driven α-CD-based [2]rotaxane with a π-extended conjugated molecular dumbbell. The intercomponent interactions responsible for the stability of this [2]rotaxane (**3b)** were revealed through several spectroscopic techniques, which helped to characterise the final material. The dumbbell-like molecule **4b** was used as a reference for the analysis of the [2]rotaxane. Interesting phenomena such as some asymmetries in the NMR signals of **3b**, as well as differentiations of the XRD patterns of **3b** in comparison with those of the dumbbell compound and of α-CD, associated with the formation of the inclusion complex **3b**, were observed and analysed. The UV–vis properties of the [2]rotaxane have shown that the rotaxanation by α-CD reduces the absorbance intensity compared to that of the free dumbbell compound. SEM and EDX analysis also proved to be really useful for the confirmation of the success of the rotaxanation reaction. Additionally through XRD, FTIR and NMR analysis, it was proved that α-CD is threaded in the region near the (–N = N–) bond as depicted in Scheme 3. Finally, the photoswitchability of the reported new [2]rotaxane, which resulted in its reversible molecular shuttling, was successfully investigated.

Experimental section

Physical measurements

NMR spectra were obtained using a Varian Gemini 300 or a Varian 600 MHz spectrometer (300 MHz ^{1}H, 75 MHz ^{13}C or 600 MHz ^{1}H). ^{1}H and ^{13}C NMR spectra were recorded either in D$_6$DMSO at 25°C (for the compounds **3b** and **4b**) or in D_2O (^{1}H) and D_2O/D$_6$DMSO (^{13}C) (compound **2**). The ROESY experiment was carried out with a spin lock mixing time of 300 ms. In all cases, the residual solvent peaks were used as internal reference

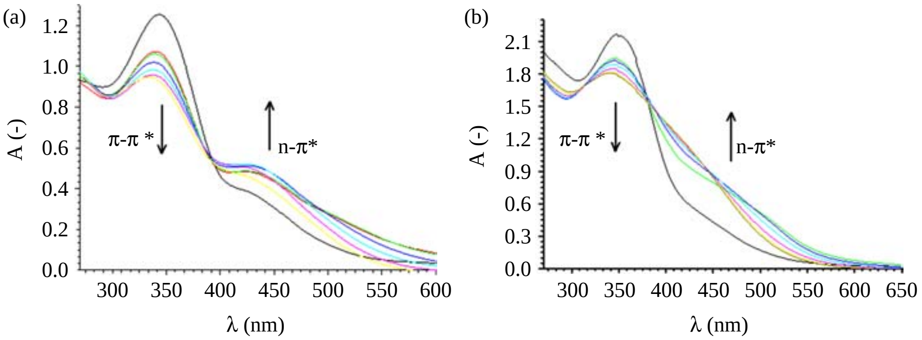

Figure 6. UV–vis spectra of (a) dumbbell compound and (b) [2]rotaxane without irradiation and after 1–6 h of irradiation.

Table 1. π–π* Band absorbances for **3b** before and after irradiation recorded in DMSO.

t	A_p	A_t	$\lvert A_t - A_p\rvert / A_t$	% E–Z	$\ln(\lvert A_t - A_p\rvert / A_t)$
0	2.171	2.141	–	–	–
60	2.171	1.942	0.10	10.25	−2.27
120	2.171	1.919	0.11	11.57	−2.15
180	2.171	1.884	0.13	13.64	−1.99
240	2.171	1.849	0.15	15.79	−1.84
300	2.171	1.814	0.18	18.03	−1.71
360	2.171	1.801	0.20	20.54	−1.58

Table 2. π–π* Band absorbances for **4b** before and after irradiation recorded in DMSO.

t	A_p	A_t	$\lvert A_t - A_p\rvert / A_t$	% E–Z	$\ln(\lvert A_t - A_p\rvert / A_t)$
0	1.254	1.254	–	–	–
60	1.254	1.069	0.17305893	17.31	−1.75412309
120	1.254	1.055	0.18862559	18.86	−1.66799122
180	1.254	1.014	0.23668639	23.67	−1.44101926
240	1.254	0.976	0.28483607	28.48	−1.25584147
300	1.254	0.940	0.33404255	33.40	−1.09648689
360	1.254	0.900	0.39333333	39.33	−0.93309785

(2.5 ppm for D_6DMSO concerning Proton Magnetic Resonance (PMR), and 39.52 ppm for D_6DMSO concerning ^{13}C NMR; 4.79 ppm for D_2O concerning NMR and 39.39 ppm for D_6DMSO in D_2O concerning ^{13}C NMR) (*21*). Abbreviations used for multiplicity in the text: s = single; d = doublet; pd = pseudo doublet and m = multiplet. IR spectra were recorded on a Perkin-Elmer Spectrum 1 FTIR spectrophotometer in the solid state (without any preparation of the samples) using the attenuated total reflectance technique (ATR) in the region 600–4000 cm^{-1}. UV–vis spectra were recorded using a Varian CARY 1E UV–vis spectrophotometer at 25 ± 1°C in DMSO solutions. The concentrations of the solutions used were about 50 ppm and they were prepared right before each measurement. Electrospray ionisation ESI-HR-MS spectra were obtained on a Waters, Inc. Q-TOF Premier Mass Spectrometer (High Resolution Mass Spectroscopy facility, Iowa University, Iowa, USA). Melting points were determined in open capillary tubes using a Gallenkamp HFB-595 melting point apparatus and are uncorrected. Powder XRD measurements were carried out using a Siemens D5000 diffractometer using Cu Ka1, radiation $\lambda = 1.5405$ Å, and a graphite monochromator. Finally, SEM images and EDX measurements were obtained using a FEI Quanta 200 SE-Microscope. For the photoswitchability investigation, all spectra were recorded using a Varian CARY 1E UV–vis spectrophotometer at 25°C, before and after illumination by external light irradiation with a 365 nm UV light lamp. The UV light sources were obtained from a low pressure Mercury lamp, and the light beam with a wavelength of about 365 nm, achieved through suitable filters, in a sealed Ar-saturated 1 cm quartz cell. The distance between the lamp and the sample cell was about 5 cm (*37*).

Materials and procedures

Fluoro-2,4-dinitrobenzene and 4,4′-ADA were purchased from ACROS Organics, α-CD was obtained from Fluka in 99.0% purity and was dried *in vacuo* over P_2O_5 prior to use, and finally 4,4′-bipyridine was obtained from Fluka as well, and it was used without further purification. The solvents used were degassed for several minutes with argon before use. Water was purified with a Barnstead EASYpure RF compact ultrapure water system and then distilled twice. In all cases of complex formation reactions, the reaction mixture was kept under argon atmosphere. All the reactions were monitored through thin layer chromatography (TLC). The silica gel TLC plates were ALUGRAM SIL G/UV254 purchased from Macherey-Nagel. TLC was also used in order to check the absence of unreacted α-CD, or of the unreacted linear molecules in the final materials. The final products were dried under vacuum over anhydrous $CaCl_2$ or P_2O_5 in case of CD complexes, for several days until they were brought to a constant weight.

Synthesis of linear compound **2**

Compound **1** (1.01 g, 2.83 mmol) and 4,4′-ADA (0.3 g, 1.41 mmol) were mixed in a round flask in molar proportion 2:1, respectively, and heated overnight without solvent in an oil bath regulated at 150–170°C. The solid mass was then dissolved in MeOH and compound **2** was precipitated by adding Et_2O and then filtered, washed with Et_2O and dried *in vacuo*. Red brown powder (0.54 g, 68%), mp: > 250°C; ^{1}H NMR (300 MHz, D_2O, 26°C): $\delta = 9.43$ (d, $J = 6.3$ Hz, 4H; C_5H_5N), 8.97 (d, $J = 6.3$ Hz, 4H; C_5H_5N), 8.74 (d, $J = 7.2$ Hz, 4H; C_5H_5N), 8.35 (d, $J = 8.4$ Hz, 4H; Ph), 8.29 (d, $J = 4.8$ Hz, 4H; C_5H_5N), 8.18 (d, $J = 8.1$ Hz, 4H; Ph); ^{13}C NMR (75 MHz, D_2O/D_6DMSO, 26°C): $\delta = 153.48$, 152.78, 150.80, 145.48, 144.22, 140.86, 126.56, 125.37, 124.27, 122.29. MS-ESI (*m/z*): calculated for $C_{32}H_{25}N_6Na$ ($M - 2Cl + Na + H$), 563.57 found: 563.49.

Synthesis of [2]rotaxane ***3b***

Compound **2** (0.1 g, 0.177 mmol), α-CD (0.862 g, 0.887 mmol) and fluoro-2,4-dinitrobenzene (0.33 g, 1.77 mmol) were mixed in proportion 1:5:10 (molar) in water (25 ml). The reaction mixture was degassed under an atmosphere of argon and stirred at ~30°C for 7 days. The mixture was then washed several times with chloroform (removal of unreacted fluoro-2,4-dinitrobenzene), and then a saturated aqueous solution of NH_4PF_6 was added to induce precipitation of compound **3b** which was filtered and washed with water several times. Red solid (0.23 g, 54%), mp: 238°C (dec.); ^{1}H NMR (300 MHz, D_6DMSO, 26°C): $\delta = 9.85$ (d, $J = 5.4$ Hz, 2H; C_5H_5N), 9.75 (m, 4H), 9.68 (d, $J = 6.3$ Hz, 2H; C_5H_5N), 9.21 (m, 8H), 9.07 (m, 6H), 8.79 (d, $J = 7.5$ Hz, 1H), 8.47 (d, $J = 8.7$ Hz, 1H), 8.30 (d, $J = 5.4$ Hz, 2H), 8.18 (m, 4H; arom.), 5.52 (d, $J = 6.3$ Hz, 6H; α-CD), 5.39 (s, 6H; α-CD), 4.83 (s, 6H; α-CD), 4.48 (s, 6H; α-CD), 3.60 (m, 36H; α-CD); ^{13}C NMR (75 MHz, D_6DMSO, 26°C): $\delta = 149.48$, 147.62, 147.32, 145.99, 144.24, 143.19, 143.18, 143.05, 141.96, 138.38, 133.84, 131.96, 130.41, 126.81, 124.13, 121.63, 101.87, 81.35, 73.42, 72.01, 59.6; HR-MS-ESI (*m/z*): calculated for $C_{80}H_{90}N_{10}O_{38}$ ($M - 4PF_6 + 1H$), 1798.5412 found: 1798.5418. UV–vis (DMSO, λ_{nm} ($\log\epsilon_{max}$)): 351 (4.656), (π–π*); IR (ATR): $\nu = 3381$ (ν_{OH}), 1605 ($\nu_{-N=N-}$), 1548 (ν_{NO2}), 1446, 1347 (ν_{NO2}) cm^{-1}.

Synthesis of dumbbell ***4b***

Compound **2** (0.1 g, 0.177 mmol) and fluoro-2,4-dinitrobenzene (0.33 g, 1.77 mmol) were mixed in proportion 1:10 (molar) in water (25 ml) and stirred at ~30°C for 7 days. The method used was exactly the same as in case of compound **3b**. Red solid (0.2 g, 80%), mp: > 250°C; ^{1}H NMR (300 MHz, D_6DMSO, 26°C): $\delta = 9.83$ (d, $J = 5.4$ Hz, 3H, C_5H_5N), 9.74 (d, $J = 5.4$ Hz, 3H, C_5H_5N), 9.58 (d, $J = 6.3$ Hz, 2H), 9.19 (m, 4H), 9.11 (m, 4H), 8.94 (d, $J = 0.5$ Hz, 2H), 8.84 (d, $J = 5.4$ Hz, 2H), 8.46 (m, 2H), 8.39 (m, 3H), 8.32 (m, 3H), 8.17 (pd,2H); ^{13}C NMR (75 MHz, D_6DMSO, 26°C): $\delta = 153.086$, 151.08, 149.41, 147.37, 146.16, 145.01, 143.08, 132.09, 130.39, 127.02, 126.75, 126.61, 125.43, 124.42, 122.23, 121,58; HR-MS-ESI (*m/z*): calculated for $C_{44}H_{30}N_{10}O_8$ ($M - 4PF_6 + 1H$), 826.2242 found: 826.2245. UV–vis (DMSO, λ_{nm} ($\log\epsilon_{max}$)): 337 (4.569), (π–π*); IR (ATR): $\nu = 1595$ ($\nu_{-N=N-}$), 1522 (ν_{NO2}), 1484, 1373 (ν_{NO2}), 1218 cm^{-1}.

References

(1) Amabilino, D.B.; Stoddart, J.F. *Chem. Rev.* **1995**, *95*, 2725–2828.

(2) Taira, T.; Suzaki, Y.; Osakada, K. *Chem. Asian J.* **2008**, *3*, 895–902.

(3) Raymo, F.M.; Stoddart, J.F. *Chem. Rev.* **1999**, *99*, 1643–1664.

(4) Armaroli, N.; Balzani, V.; Collin, J.-P.; Gaviña, P.; Sauvage, J.-P.; Ventura, B. *J. Am. Chem. Soc.* **1999**, *121*, 4397–4408.

(5) Benniston, A.C.; Harriman, A. *Angew. Chem. Int. Ed. Engl.* **1993**, *32*, 1459–1461.

(6) Collier, C.P.; Wong, E.W.; Belohradsky, M.; Raymo, F.M.; Stoddart, J.F.; Kuekes, P.J.; Williams, R.S.; Heath, J.R. *Science* **1999**, *285*, 391–394.

(7) Collier, C.P.; Belohradsky, M.; Raymo, F.M.; Stoddart, J.F.; Heath, J.R. *J. Am. Chem. Soc.* **2000**, *122*, 5831–5840.

(8) Leigh, D.A.; Morales, M.Á.F.; Pérez, E.M.; Wong, J.K.Y.; Saiz, C.G.; Slawin, A.M.Z.; Carmichael, A.J.; Haddleton, D.M.; Brouwer, A.M.; Buma, W.J.; Wurpel, G.W.H.; León, S.; Zerbetto, F. *Angew. Chem. Int. Ed.* **2005**, *44*, 3062–3067.

(9) Qu, D.-H.; Wang, Q.-C.; Tian, H. *Angew. Chem. Int. Ed.* **2005**, *44*, 5296–5299.

(10) Qu, D.-H.; Ji, F.-Y.; Wang, Q.-C.; Tian, H. *Adv. Mater.* **2006**, *18*, 2035–2038.

(11) Murakami, H.; Kawabuchi, A.; Kotoo, K.; Kunitake, M.; Nakashima, N. *J. Am. Chem. Soc.* **1997**, *119*, 7605–7606.

(12) Asakawa, M.; Higuchi, M.; Mattersteig, G.; Nakamura, T.; Pease, A.R.; Raymo, F.M.; Shimizum, T.; Stoddart, J.F. *Adv. Mater.* **2000**, *12*, 1099–1102.

(13) Kay, E.R.; Leigh, D.A.; Zerbetto, F. *Angew. Chem. Int. Ed.* **2007**, *46*, 72–191.

(14) Feringa, B.L. *Acc. Chem. Res.* **2001**, *34*, 504–513.

(15) Taylor, P.N.; Connell, M.J.O.; McNeill, L.A.; Hall, M.J.; Aplin, R.T.; Anderson, H.L. *Angew. Chem. Int. Ed.* **2000**, *39*, 3456–3460.

(16) Cacialli, F.; Wilson, J.S.; Michels, J.J.; Daniel, C.; Silva, C.; Friend, R.H.; Severin, N.; Samorì, P.J.; Rabe, P.; O'Connell, M.J.; Taylor, P.N.; Anderson, H.L. *Nat. Mater.* **2002**, *1*, 160–164.

(17) Taylor, P.N.; Hagan, A.J.; Anderson, H.L. *Org. Biomol. Chem.* **2003**, *1*, 3851–3856.

(18) Willner, I.; Pardo-Yissar, V.; Katz, E.; Ranjit, K.T. *J. Electroanal. Chem.* **2001**, *497*, 172–177.

(19) Yang, Y.-W.; Chen, Y.; Liu, Y. *Inorg. Chem.* **2006**, *45*, 3014–3022.

(20) Harada, A. *Acc. Chem. Res.* **2001**, *34*, 456–464.

(21) Gottlieb, H.E.; Kotlyar, V.; Nudelman, A. *J. Org. Chem.* **1997**, *62*, 7512–7515.

(22) Coe, B.J.; Harries, J.L.; Helliwell, M.; Jones, L.A.; Asselberghs, I.; Clays, K.; Brunschwig, B.S.; Harris, J.A.; Garin, J.; Orduna, J. *J. Am. Chem. Soc.* **2006**, *128*, 12192–12204.

(23) Papadakis, R.; Tsolomitis, A. *J. Phys. Org. Chem.* **2009**, *22*, 515–521.

(24) Nepogodiev, S.A.; Stoddart, J.F. *Chem. Rev.* **1998**, *98*, 1959–1976.

(25) Papadakis, R.; Deligkiozi, I.; Tsolomitis, A. *Anal. Bioanal. Chem.* **2010**, *397*, 2253–2259.

(26) Li, S.; Purdy, W.C. *Chem. Rev.* **1992**, *92*, 1457–1470.

(27) Ma, X.; Wang, Q.; Qu, D.; Xu, Y.; Ji, F.; Tian, H. *Adv. Funct. Mater.* **2007**, *17*, 829–837.

(28) Harada, A.; Suzuki, S.; Okada, M.; Kamachi, M. *Macromolecules* **1996**, *29*, 5611–5614.

(29) Liu, Y.; You, C.C.; Zhang, H.Y.; Kang, S.-Z.; Zhu, C.-F.; Wang, C. *Nano Lett.* **2001**, *1*, 613–616.

(30) Okumura, H.; Kawaguchi, Y.; Harada, A. *Macromolecules* **2001**, *34*, 6338–6343.

(31) Briquet, L.; Vercauteren, D.P.; Andre, J.-M.; Perpete, E.A.; Jacquemin, D. *Chem. Phys. Lett.* **2007**, *435*, 257–262.

(32) Park, J.; Koh, J. *Dyes Pigment* **2009**, *82*, 347–352.

(33) Rajamohan, R.; Nayaki, S.K.; Swaminathan, M. *Spectrochim. Acta A.* **2008**, *69*, 371–377.

(34) Murakami, H.; Kawabuchi, A.; Kotoo, K.; Kunitake, M.; Nakashima, N. *J. Am. Chem. Soc.* **1997**, *119*, 7605–7606.

(35) Stanier, C.A.; Alderman, S.J.; Claridge, T.D.W.; Anderson, H.L. *Angew. Chem. Int. Ed.* **2002**, *41*, 1769–1772.

(36) Ma, X.; Tian, H. *Chem. Soc. Rev.* **2010**, *39*, 70–80.

(37) Murakami, H.; Kawabuchi, A.; Matsumoto, R.; Ido, T.; Nakashima, N. *J. Am. Chem. Soc.* **2005**, *127*, 15891–15899.

(38) Wang, Q.; Qu, D.H.; Ren, J.; Chen, K.; Tian, H. *Angew. Chem. Int. Ed.* **2004**, *43*, 2661–2665.

(39) Qu, D.H.; Wang, Q.; Ma, X.; Tian, H. *Chem. Eur. J.* **2005**, *11*, 5929–5937.

(40) Kudernac, T.; Katsonis, N.; Browne, W.R.; Feringa, B.L. *J. Mater. Chem.* **2009**, *19*, 7168–7177.

(41) Nakagawa, M.; Rikukawa, M.; Watanabe, M.; Sanui, K.; Ogata, N. *Bull. Chem. Soc. Jpn.* **1997**, *70*, 737–744.